2950 Niles Road, St. Joseph, MI 49085-9659, USA
269.429.0300 fax 269.429.3852 hq@asabe.org www.asabe.org

An ASABE Meeting Presentation

Paper Number: 09-7166

Material and Interaction Properties of Selected Grains and Oilseeds for Modeling Discrete Particles

Josephine M. Boac, Graduate Student
Kansas State University, 129 Seaton Hall, Manhattan, Kansas, jmboac@ksu.edu.

Mark E. Casada, Ph.D., P.E., Lead Scientist and Agricultural Engineer
USDA-ARS GMPRC EWERU, 1515 College Ave., Manhattan, Kansas, casada@ksu.edu.

Ronaldo G. Maghirang, Ph.D., Professor
Kansas State University, 129 Seaton Hall, Manhattan, Kansas, rmaghir@ksu.edu.

Joseph P. Harner, III, Ph.D., Professor, Interim Department Head
Kansas State University, 129 Seaton Hall, Manhattan, Kansas, jharner@ksu.edu.

Written for presentation at the
2009 ASABE Annual International Meeting
Sponsored by ASABE
Grand Sierra Resort and Casino
Reno, Nevada
June 21 – June 24, 2009

Abstract. *Experimental investigations of grain flow can be expensive and time consuming, but computer simulations can reduce the large effort required to evaluate the flow of grain in handling operations. Published data on material and interaction properties of selected grains and oilseeds relevant to discrete element method (DEM) modeling were reviewed. Material properties include grain kernel shape, size, and distribution; Poisson's ratio; shear modulus; and density. Interaction properties consist of coefficients of restitution, static friction, and rolling friction. Soybeans were selected as the test material for DEM simulations to validate the model fundamentals using material and interaction properties. Single- and multi-sphere soybean particle shapes, comprised of one to four overlapping spheres, were compared based on DEM simulations of bulk properties (bulk density and angle of repose). A single-sphere particle model best simulated soybean kernels in the bulk property tests. The best particle model had a particle coefficient of restitution of 0.6; particle static friction of 0.45 for soybean-soybean contact (0.30 for soybean-steel interaction); particle rolling friction of 0.05; normal particle size distribution with standard deviation factor of 0.4; and particle shear modulus of 1.04 MPa.*

Keywords. Discrete element method, simulation, material properties, interaction properties, soybeans, corn, wheat, sunflower, canola, sorghum, rice, barley, oats, single-sphere particle, multi-sphere particle

Introduction[1]

Physical characteristics are important in analyzing the behavior of grains in handling operations (Mohsenin, 1986). Bulk handling behavior of the grains can be studied experimentally, but large-scale investigations of grain flow can be expensive and time consuming. On the other hand, computer simulations can reduce the large effort required to evaluate the flow of grain in handling operations.

Recently, grain segregation and identity preservation operations have become important as grain handlers respond to an increased use of specialty grain (Berruto and Maier, 2001; Herrman et al., 2001, 2002). However, limited studies have been conducted to quantify the commingling that may occur during grain handling in grain elevators (Hurburgh, 1999; Ingles et al., 2003, 2006) and with farm equipment (Greenlees and Shouse, 2000; Hirai et al., 2006; Hanna et al., 2006). Limited data on grain commingling during handling in grain elevators (Ingles et al., 2003, 2006) make it difficult to accurately predict levels of impurities that would propagate through grain handling systems. Thus, a validated mechanistic model for predicting grain commingling in various types of elevator equipment will be valuable for extending the knowledge of grain commingling beyond current experimental studies.

Different modeling techniques such as continuum models and discrete element models (Wightman et al., 1998) have potential to simulate grain commingling in elevator equipment. The discrete element method (DEM) is considered one of the most promising techniques to simulate movement of individual grain kernels (Wightman et al., 1998) in bucket elevator equipment. DEM is an explicit numerical scheme in which particle interaction is monitored contact by contact and the motion of individual particles is modeled (LoCurto et al., 1997). This explicit scheme requires small time steps, resulting in potential problems with developing realistic models that can run in a reasonable time on current computers. The model must use a critical time increment that achieves stability and simulates the true physics with a manageable number of iterations or calculations (O'Sullivan and Bray, 2004; Li et al., 2005).

Relevant grain physical properties must be known to accurately simulate grain handling operations. The objectives of this study were (1) to review the published physical properties of grains and oilseeds needed to model grain commingling in DEM, and (2) to develop and validate an appropriate particle model for one test seed based on these physical properties. Soybeans were chosen as the test seed due to their almost spherical shape for simplicity of modeling. Additionally, other major seeds with non-spherical shapes (e.g., corn, wheat) were also reviewed in this study. Their physical properties can be used for future DEM modeling.

Physical Properties of Grains and Oilseeds

Different DEM models have used varying parameters for simulation modeling. The most widely used parameters can be divided into two categories: material properties and interaction properties (Mohsenin, 1986; Vu-Quoc et al., 2000; Raji and Favier, 2004a, 2004b). Material properties may be defined as intrinsic characteristics of the particle (i.e., grain kernels) that is being modeled. Among material properties critical as inputs in DEM modeling are shape, size distribution, density, Poisson's ratio, and shear modulus. Interaction properties are characteristics exhibited by the particle in relation to its contact with boundaries, surfaces, and

---

[1] Mention of trade names or commercial products in this article is solely for the purpose of providing specific information and does not imply recommendation or endorsement by the U.S. Department of Agriculture.

other (or same) particles. Interaction properties, vital in DEM modeling, are coefficients of restitution, and static and rolling friction (LoCurto et al., 1997; Chung et al., 2004). Grain material and interaction properties available in the literature are summarized in Table 1.

Particle Shape and Particle Size

Shape and size are inseparable physical properties in a grain kernel. In defining shape, some dimensional parameters of the grain must be measured. Mohsenin (1986) and Nelson (2002) reported measuring three orthogonally oriented dimensions of 50 kernels randomly selected from a grain lot to determine kernel shape and size. The volume was taken as one of the parameters defining kernel shape and the three mutually perpendicular axes were taken as a measure of kernel size.

Particle Density

Particle density (ρ_p) of the grain is determined by measuring the volume occupied by the kernels in a known sample weight, randomly taken from each grain lot. Nelson (2002) measured the volume of an approximately 20- to 25-g sample with a Beckman model 930 air-comparison pycnometer. Kernel density was calculated by dividing the weighed mass by the measured volume. The number of kernels in the sample weighed for pycnometer measurements was manually counted to determine mean kernel weight and volume. Table 1 lists published ranges of particle density for different grains and oilseeds.

Particle Poisson's Ratio and Particle Shear Modulus

Poisson's ratio (ν) is the absolute value of the ratio of transverse strain (perpendicular to the axis) to the corresponding axial strain (parallel to the longitudinal axis) resulting from uniformly distributed axial stress below the proportional limit of the material (Mohsenin, 1986). Based on Hooke's law and together with Poisson's ratio, shear modulus or modulus of rigidity (G) for an elastic, homogenous, and isotropic material is the ratio of the stress component tangential to the plane on which the forces acts (i.e., shear stress) over its strain. Shear modulus defined in terms of Poisson's ratio and Young's modulus or modulus of elasticity (E) is given by Equation 1.

$$G = \frac{E}{2 + 2\nu} \qquad (1)$$

Several values of Poisson's ratio and elastic or Young's modulus for different grains and oilseeds were cited in the literature (Table 1). ASAE Standards S368.4 (2006b) enumerated values of Poisson's ratio and apparent modulus of elasticity for soybeans, corn, and wheat. The equations for apparent modulus of elasticity are based on Hertz equations for contact stresses used in solid mechanics, which assume that deformations are small and the material being compressed is elastic. They are, however, useful for making comparisons of the deformation behavior of viscoelastic materials, like grains, when the deformations and loading rates are similar for all samples tested.

For soybeans (Misra and Young, 1981) and wheat (Arnold and Roberts, 1969), apparent moduli of elasticity were calculated based on the parallel plate contact method. For corn (Shelef and Mohsenin, 1969), the elastic modulus was obtained with a method using a spherical indenter on a curved surface.

Table 1. Range of published physical properties of grains and oilseeds.

Grain/ Oilseed Kernels		Soybean		Corn		Wheat	
Parameters							
Moisture Content (%) wb		6.9 - 16.7	b, j, k, p, s, t, y, z	6.7 - 25.0	e, f, h, k, s, y, z, aa	6.2 - 20.0	e, f, g, k, s, y, z, aa
Particle Length (mm), *l*		7.0 - 8.2	q, s, t, y	9.4 - 20.3	k, s, u, y, ac	5.5 - 7.3	k, s, y
Particle Width (mm), w		6.1 - 6.7	q, s, t, y	8.0 - 16.4	k, s, u, y, ac	2.6 - 3.8	k, s, y
Particle Thickness (mm), *h*		5.5 - 5.9	q, s, t, y	4.0 - 12.8	k, s, u, y, ac	2.4 - 3.5	k, s, y
Particle Equivalent Diameter (mm), d_e		6.0	k, w	8.0	k	3.6 - 4.1	k
Particle Radius (mm), r_e		3.0	k, w	4.0	k	1.8 - 2.1	k
Particle Mass (mg), *m*		100 - 200	q, r, s, t, y	250 - 349.7	e, k, *l*, s, u, y,	26 - 51	k, *l*, r, s, y
Particle Volume (mm^3), *V*		134.1 - 152.8	s	274	s	18.5 - 28.6	s
Particle Density (kg/m^3), ρ_p		1130 - 1325.2	s, w, y, z	1270 - 1396.5	k, s, y, z, ac	1290 - 1430	k, s, y, z
Bulk Density (kg/m^3), ρ_b		705 - 876	i, p, s, y, z	661 - 810	i, k, *l*, s, y, z	690 - 823.2	i, k, *l*, s, y, z
Particle Poisson Ratio, *v*		0.08 - 0.4134	j, q, t, w, y	0.17 - 0.4	h, k, v, y, aa, ac	0.16 - 0.42	g, y, aa
Particle Elastic Modulus (MPa), *E*		31.2 - 176.9	j, t, w, y	10.9 - 2320	h, v, y, aa, ac	10 - 2834	g, y
Particle Shear Modulus (MPa), *G*		13.3 - 63.2	j, t, w, y	4.5 - 828.6	h, v, y, aa, ac	4.2 - 997.9	g, y
Particle Restitution Coefficient, *e*	generic	0.5, 0.7	w, q	-		-	
	with aluminum	0.6, 0.7	p	-		-	
	with acrylic	-		0.59	aa	-	
Particle Static Friction Coefficient, μ_s	with self (grain)	0.267, 0.55	q, d, k	0.52, 0.51	a, d, k	0.47, 0.53	a, b, d, k
	with galvanized sheet (or sheet metal)	0.18 - 0.27	f, k, y	0.20 - 0.34	f, k, y,	0.10 - 0.44	f, k, y
	with steel (or stainless steel)	0.223 - 0.247, 0.37	y, d, k	0.235 - 0.76	a, d, e, k, v, y	0.248 - 0.55	a, b, d, e, k, y
	with transparent perspex	0.30	w	-		-	
	with aluminum	-		0.226 - 0.276	v	-	
	with acrylic	-		0.34	t	-	
	with glass	0.328	q				
Bulk Static Angle of Repose (degree)	for filling or piling	16	d, k	16	d, k	16	d, k
	for emptying or funneling	29 - 33	d, k, y	23.1 - 34.7	d, k, y	23.8 - 38.1	d, k, y
Bulk Angle of Internal Friction (degree)		29.2 - 31	y	26.1 - 35.1	y	25.4 - 36.0	y

[*] Unhulled seed or paddy
[**] Dehulled kernel
[+] Oil type
[++] Non-oil type

[a] Airy (1898)
[b] Jamieson (1903)
[c] Kramer (1944)
[d] Stahl (1950)
[e] Lorenzen (1957)
[f] Brubaker and Pos (1965)
[g] Arnold and Roberts (1969)
[h] Shelef and Mohsenin (1969)
[i] Henderson and Perry (1976)
[j] Misra and Young (1981)
[k] Mohsenin (1986)
[l] Hoseney and Faubion (1992)
[m] Bilanski et al. (1994)
[n] Shroyer et al. (1996)
[o] Gupta and Das (1997)
[p] LoCurto et al. (1997)
[q] Vu-Quoc et al. (2000)
[r] McLelland and Miller (2001)
[s] Nelson (2002)
[t] Zhang and Vu-Quoc (2002)
[u] Watson (2003)
[v] Chung et al. (2004)
[w] Raji and Favier (2004a, 2004b)
[x] Calisir et al. (2005)
[y] Molenda and Horabik (2005)
[z] ASABE Standards (2006a) - D241.4
[aa] ASAE Standards (2006b) - S368.4
[ab] Boyles et al. (2006)
[ac] Chung and Ooi (2008)

Table 1. Range of published physical properties of grains and oilseeds. (cont.)

Grain/ Oilseed Kernels Parameters		Grain Sorghum		Rice		Barley	
Moisture Content (%) wb		9.2 - 11.2	k, s, z	8.6 - 15.7	c, d, k, s, z	7.5 - 20.0	e, f, k, s, y, z
Particle Length (mm), *l*		4.3, 4.5	k, s	5.3 - 8.9**, 7.6 - 9.8	k, s	7.9 - 10.9	k, s, y
Particle Width (mm), w		4.1	k, s	2.1 - 2.9**, 2.5 - 3.6	k, s	2.9 - 3.8	k, s, y
Particle Thickness (mm), *h*		2.8, 3.4	k, s	1.7 - 2.0**, 2.1 - 2.5	k, s	2.2 - 3.0	k, s, y
Particle Equivalent Diameter (mm), d_e		3.5	k	3.3 - 3.5	k	3.7 - 4.2	k
Particle Radius (mm), r_e		1.8	k	1.7 - 1.8	k	1.9 - 2.1	k
Particle Mass (mg), *m*		28 - 33.2	k, *l*, s	17.5 - 24.9**, 25 - 29.1	k, *l*, s	25.1 - 53.9	k, s, y, z
Particle Volume (mm^3), *V*		24.7	s	12 - 18**	s	19.7 - 25.9	s
Particle Density (kg/m^3), ρ_p		1220 - 1344	k, s, z	1382-1462**, 1110-1120*, 1360-1390	k, s, z	1130 - 1420	k, s, y, z
Bulk Density (kg/m^3), ρ_b		643.5 - 775	i, k, *l*, s, z	641-851**, 579*, 573.2-579	i, k, *l*, s, z	566 - 691	i, k, *l*, s, y, z
Particle Poisson Ratio, *v*		-		-		0.14 - 0.20	y
Particle Elastic Modulus (MPa), *E*		-		-		8.0 - 15.8	y
Particle Shear Modulus (MPa), *G*		-		-		3.3 - 6.87	y
Particle Restitution Coefficient, *e*	generic	-		-		-	
	with aluminum	-		-		-	
	with acrylic	-		-		-	
Particle Static Friction Coefficient, μ_s	with self (grain)	0.65	d, k	0.68*, 0.73*	c, d, k	0.51, 0.53	a, d, k
	with galvanized sheet (or sheet metal)	-		0.40 - 0.45*	c, k	0.17 - 0.352	f, k, y
	with steel (or stainless steel)	0.37	d, k	0.48*	d, k	0.226 - 0.40	a, d, e, k, y
	with transparent perspex	-		-		-	
	with aluminum	-		-		-	
	with acrylic	-		-		-	
	with glass						
Bulk Static Angle of Repose (degree)	for filling or piling	20	d, k	20*	d, k	16	d, k
	for emptying or funneling	33	d, k	36*	d, k	26.1 - 32.9	d, k, y
Bulk Angle of Internal Friction (degree)		-		-		27.4 - 33.7	y

* Unhulled seed or paddy
** Dehulled kernel
\+ Oil type
\++ Non-oil type

[a] Airy (1898)
[b] Jamieson (1903)
[c] Kramer (1944)
[d] Stahl (1950)
[e] Lorenzen (1957)
[f] Brubaker and Pos (1965)
[g] Arnold and Roberts (1969)
[h] Shelef and Mohsenin (1969)
[i] Henderson and Perry (1976)
[j] Misra and Young (1981)
[k] Mohsenin (1986)
[l] Hoseney and Faubion (1992)
[m] Bilanski et al. (1994)
[n] Shroyer et al. (1996)
[o] Gupta and Das (1997)
[p] LoCurto et al. (1997)
[q] Vu-Quoc et al. (2000)
[r] McLelland and Miller (2001)
[s] Nelson (2002)
[t] Zhang and Vu-Quoc (2002)
[u] Watson (2003)
[v] Chung et al. (2004)
[w] Raji and Favier (2004a, 2004b)
[x] Calisir et al. (2005)
[y] Molenda and Horabik (2005)
[z] ASABE Standards (2006a) - D241.4
[aa] ASAE Standards (2006b) - S368.4
[ab] Boyles et al. (2006)
[ac] Chung and Ooi (2008)

Table 1. Range of published physical properties of grains and oilseeds. (cont.)

Grain/ Oilseed Kernels Parameters		Oats		Sunflower		Canola	
Moisture Content (%) wb		8.5 -20.0	f, k, s, y, z	3.9 - 16.7	o, s	4.5 - 19.3	m, s, x, y, z
Particle Length (mm), *l*		10.2 - 14.9	k, s, y	9.5[*], 8.3[**], 10.7[+], 14.4[++]	o, s	1.6 - 2.305	s, x, y
Particle Width (mm), w		2.7 - 3.1	k, s, y	5.1[*], 4.1[**], 5.2[+], 8.1[++]	o, s	1.4, 1.7	s, y
Particle Thickness (mm), *h*		2.1 - 2.6	k, s, y	3.3[*], 2.4[**], 3.1[+], 4.6[++]	o, s	1.7	y
Particle Equivalent Diameter (mm), d_e		3.5 - 3.8	k	5.4[*], 4.3[**]	o	1.824 - 2.0	m, w, x
Particle Radius (mm), r_e		1.8 - 1.9	k	2.7[*], 2.15[**]	o	0.9 - 1.0	m, w, x
Particle Mass (mg), *m*		28.1 - 39.5	k, *l*, s, y	49[*], 34[**], 59.5-126[+], 115.8[++]	o, r, s	2.9 - 6.6	r, s, x, y
Particle Volume (mm^3), *V*		21.4, 26.8	s	58.2[+], 105.4[++]	s	2.7 - 5.225	s, x
Particle Density (kg/m^3), ρ_p		950 - 1397	k, s, y, z	706-765[*], 1050-1250[**], 1023[+], 1099[++]	o, s	1053 - 1150	w, s, y, z
Bulk Density (kg/m^3), ρ_b		412 - 576	k, *l*, s, y, z	434-462[*], 574-628[**], 386-412[+], 309-339[++], 361.2	n, o, s, z	640 - 671	s, y, z
Particle Poisson Ratio, *v*		0.14 - 0.21	y	-		0.09 - 0.4	m, w, y
Particle Elastic Modulus (MPa), *E*		8.3 - 20.6	y	-		5.7 - 50.1	m, w, y
Particle Shear Modulus (MPa), *G*		3.52 - 8.80	y	-		2.57 - 17.9	m, w, y
Particle Restitution Coefficient, *e*	generic	-		-		0.6	w
	with aluminum	-		-		-	
	with acrylic	-		-		-	
Particle Static Friction Coefficient, μ_s	with self (grain)	0.53, 0.62	a, d, k	-		0.5	w
	with galvanized sheet (or sheet metal)	0.18 - 0.41	f, k, y	0.40 - 0.58[*], 0.43 - 0.81[**]	o	0.211 - 0.322	x, y
	with steel (or stainless steel)	0.233 - 0.45	a, d, k, y	-		0.234 - 0.301	y
	with transparent perspex	-		-		0.30	w
	with aluminum	-		-		-	
	with acrylic	-		-		-	
	with glass						
Bulk Static Angle of Repose (degree)	for filling or piling	18	d, k	-		-	
	for emptying or funneling	27.7 - 35.1	d, k, y	34 - 41[*], 27 - 38[**]	o	22 - 29.8	y, ab
Bulk Angle of Internal Friction (degree)		21.0 - 28.1	y	-		24.2 - 35.5	y

[*] Unhulled seed or paddy
[**] Dehulled kernel
[+] Oil type
[++] Non-oil type

[a] Airy (1898)
[b] Jamieson (1903)
[c] Kramer (1944)
[d] Stahl (1950)
[e] Lorenzen (1957)
[f] Brubaker and Pos (1965)
[g] Arnold and Roberts (1969)
[h] Shelef and Mohsenin (1969)
[i] Henderson and Perry (1976)
[j] Misra and Young (1981)
[k] Mohsenin (1986)
[l] Hoseney and Faubion (1992)
[m] Bilanski et al. (1994)
[n] Shroyer et al. (1996)
[o] Gupta and Das (1997)
[p] LoCurto et al. (1997)
[q] Vu-Quoc et al. (2000)
[r] McLelland and Miller (2001)
[s] Nelson (2002)
[t] Zhang and Vu-Quoc (2002)
[u] Watson (2003)
[v] Chung et al. (2004)
[w] Raji and Favier (2004a, 2004b)
[x] Calisir et al. (2005)
[y] Molenda and Horabik (2005)
[z] ASABE Standards (2006a) - D241.4
[aa] ASAE Standards (2006b) - S368.4
[ab] Boyles et al. (2006)
[ac] Chung and Ooi (2008)

Particle Coefficient of Restitution

Different methods have been used to determine the coefficient of restitution (Sharma and Bilanski, 1971; Smith and Liu, 1992; Yang and Schrock, 1994; LoCurto et al., 1997). Smith and Liu (1992) obtained the coefficient of restitution in three ways leading to the same value, as the (1) ratio of the normal component of impulse during compression and during restitution, (2) ratio of the normal component of approach (or impact) and separation (or rebound) velocities (Sharma and Bilanski, 1971; Yang and Schrock, 1994), and (3) ratio of work of normal components of reaction forces at the contact point during the compression phase and the work for the restitution phase (LoCurto et al., 1997).

LoCurto et al. (1997) described the coefficient of restitution as the square root of the total kinetic energy before (KE_i) and after (KE_r) collisions that did not involve tangential frictional losses. They measured the restitution coefficient of soybeans impacting aluminum, glass, and acrylic at drop heights of 151, 292, and 511 mm and at moisture contents of 10.7% and 15.5%, dry basis (db). The coefficient of restitution decreased with increased moisture content and drop height, and contact with aluminum gave the highest value. Drop and rebound heights were measured only from those soybeans that fell with minimal rotation and whose rebound trajectories were almost vertical (90 ± 1.6% to the plate). This was different from the results of Yang and Schrock (1994) which involved cases of grain kernels with and without rotation. Assuming no loss of energy except during contact, the coefficient of restitution (e) was computed as the ratio of the square root of the initial height of drop (H_i) and the height of rebound (H_r) (LoCurto et al., 1997; Zhang and Vu-Quoc, 2002):

$$e \equiv \left(\frac{KE_r}{KE_i}\right)^{\frac{1}{2}} \equiv \left(\frac{H_r}{H_i}\right)^{\frac{1}{2}} \qquad (2)$$

Particle Coefficient of Static Friction

The coefficient of friction (μ) is the ratio of the force of friction (F) to the force normal to the surface of contact (W):

$$\mu = \frac{F}{W} \qquad (3)$$

Frictional forces acting between surfaces at rest with respect to each other and those existing between the surfaces in relative motion are, respectively, called forces of static and kinetic friction. Static and kinetic coefficients of friction can be denoted by μ_s and μ_k, respectively (Mohsenin, 1986).

Several coefficients of static friction of grain-on-grain (Stahl, 1950; Mohsenin, 1986; Raji and Favier, 2004a, 2004b) and grain-on-surfaces such as sheet metal, stainless steel, acrylic, aluminum, and glass (Brubaker and Pos, 1965; Mohsenin, 1986; Gupta and Das, 1997; Chung et al., 2004; Calisir et al., 2005; Molenda and Horabik, 2005; Chung and Ooi, 2008) were published in the literature. Static friction of soybean-steel contact is 67% of that of soybean on itself (Stahl, 1950).

Particle Coefficient of Rolling Friction

The coefficient of rolling friction is defined as the ratio of the force of friction to the force normal to the surface of contact that prevents a particle from rolling. Rolling friction or resistance can be a couple (or pure moment) that may be transferred between the grains via the contacts, and this couple resists particle rotations (Jiang et al., 2005) without affecting translation. It may exist even at contacts between cylindrical grains (Bardet and Huang, 1993). The concept of taking into account rolling resistance at particle contacts is an alternative approach in DEM modeling to establish contact laws related to particle rotation (Jiang et al., 2005), instead of using non-spherical particles to inhibit particle rolling and produce a realistic rolling behavior (Rothenburg and Bathurst, 1992; Sawada and Pradhan, 1994; Ting et al., 1995; Ullidtz, 1997; Thomas and Bray, 1999; Ng, 2001; Mirghasemi et al., 2002; Mustoe and Miyata, 2001). In Jiang et al.'s (2005) micro-mechanical model, only the normal basic element, composed of a spring and dashpot in parallel with a divider series, contributes to rolling resistance at grain contact. Rolling resistance directly affects only the angular motion and not the translational motion of grains.

Zhou et al. (2002) investigated the effect of rolling friction on the angle of repose of coarse glass beads. They included coefficients of rolling friction with a base value of 0.05 (range: 0 - 0.1) on particle-to-particle contact and twice that value for particle-wall contact in their simulations. The authors found that increasing both rolling frictions increased the angle of repose. This is due to a large resistance force to the rotational motion of spheres providing an effective mechanism to consume the kinetic energy, stop the rotational motion, and lead to the formation of a “sand pile” with high potential energy (Zhou et al., 1999).

Bulk Density

Bulk density is the ratio of the mass to a given volume of a grain sample including the interstitial voids between the particles (Hoseney and Faubion, 1992; Gupta and Das, 1997). In the United States, bulk density or test weight per bushel is the weight (in lb) per Winchester bushel (2,150.42 in.^{3}) as determined using an approved device (USDA GIPSA, 2004). The USDA GIPSA (2004) method involves allowing a sufficient amount of grain from a hopper, suspended two inches above, to overflow the test weight kettle, leveling the kettle by three full-length, zigzag motions with a stroker, and weighing the grain from the kettle with an appropriate scale.

Bulk densities of most of the grain and seed lots from Nelson (2002) were tested for standard test weight using a Fairbanks Morse grain tester weight-per-bushel apparatus equipped with a one-quart measure. In Poland, Molenda and Horabik (2005) determined bulk density based on measurement of the mass of a granular material poured freely into a cylindrical container of constant volume, typically 0.25 or 1.0 L. In India, Gupta and Das (1997) measured the bulk density of sunflower seeds and kernels by filling a 500-mL container with grain from a height of 15 cm, striking the top level, and then weighing the contents. Several values of bulk density for grains and oilseeds were found in the literature (Table 1).

Bulk Angle of Repose

Angle of repose is defined as the angle with the horizontal at which the granular material will stand when piled (Mohsenin, 1986; Hoseney and Faubion, 1992). The angle of repose of grains is determined by numerous factors which include frictional forces generated by the grain flowing against itself, distribution of weight throughout the grain mass, and moisture content of the grain (Hoseney and Faubion, 1992). At least two angles of repose are commonly defined, namely the static angle of repose and the dynamic angle of repose. The dynamic angle of repose is generally smaller than the static angle of repose by at least 3 - 10º (Fowler and Wyatt, 1960).

It is generally believed that the angle of repose and the angle of internal friction are approximately the same (Mohsenin, 1986; Walton, 1994). Fowler and Chodziesner (1959) derived an empirical equation for the coefficient of angle of friction using the tilting box method. Fowler and Wyatt (1960) used a similar form of equation to define the coefficient of angle of repose. Fowler and Chodziesner (1959) noted that when the “relative roughness factor” is equal to unity (i.e., materials are sliding over themselves) and is zero (i.e., smooth surface), the angle of repose is equal to the angle of friction and is independent of the diameter of the granular material. Stewart (1968), however, showed that for at least one seed (i.e., grain sorghum), the angle of repose and the angle of internal friction are different.

There are several methods for measuring the angle of repose. The method to measure static angle includes (1) the fixed funnel and the free-standing cone, (2) the fixed-diameter cone and the funnel, and (3) the tilting box (Train, 1958). Fraczek et al. (2007) also referred to the first two methods, respectively, as “emptying,” in which the material pours through the outlet in the container bottom (or fixed funnel) to form a free-standing cone, and “piling,” in which the material flows onto a circular plate with a fixed diameter from an established height through a funnel and mounds up into a cone prism. The tilting box or inclined plane method has been used for rough rice (Kramer, 1944) and cereal grains (Burmistrova et al., 1963). In this method, the grain sample is placed inside a special box (i.e., wooden box with top side open) and placed on the upper part of an inclined plane, which has a base connected to a lifting mechanism. It is then tilted or lifted to a point at which the sample begins to move. The angle of the inclined surface when the sample began to move was measured as the angle of repose of the particular sample.

For dynamic angle, the methods include (1) the revolving cylinder (Train, 1958) and (2) that of Brown and Richards (1959). In the revolving-cylinder method, a sealed hollow cylinder with one end transparent is half-filled with granular material and is made to revolve horizontally. The free surface of the granular material forms a diametrical plane. The angle of repose is the maximum angle that this plane makes with the horizontal on rotation of the container before the sample begins to cascade. Brown and Richards’ (1959) method consists of a platform of fixed diameter immersed in a container of granular materials. The materials are allowed to escape from the box, leaving a free-standing cone of material on the platform. Fraczek et al. (2007) also named this method “submerging.” Fowler and Wyatt (1960) employed this method to measure the effect of moisture content on the angle of repose of rape seed, wheat, sand, basalt chips, polythene chips, and canary seed.

Fraczek et al. (2007) also cited a fourth method in addition to “emptying,” “piling,” and “submerging.” The method is called “pouring,” where the grain is poured into a cylinder that is then slowly lifted up to allow the grain to mound up on the base and form a characteristic cone. The angle of repose is calculated based on the cone height and the diameter of the repose base measured at four points on the cone’s perimeter. The “pouring” method is another way of determining the angle of repose that minimizes inertial effects existing when the material is dropped from a height, gains sufficient kinetic energy and inertia near the mound peak, and then flattens considerably after the fill stream is stopped (Walton and Braun, 1993).

The four abovementioned methods are based on the assumption that the mounted granular slope acquires a cone shape, but results of experimental measurements often contradicted this assumption (Fraczek et al., 2007). In only a few cases did the authors witness the forming of a cone shape. Usually, depending on the properties of the granular materials, the following deviations from the cone shape were observed: truncation of the top, and convexity and concavity of slope. The authors recommended using digital-image analysis for a more precise measurement of angle of repose. Deviations from the cone shape increased with increasing moisture content of the material as was also noted by other authors (Horabik and Lukaszuk, 2000). However, the more spherical-like the materials, the more regular the cone that forms.

Zhou et al. (2002) found that the angle of repose of mono-sized coarse glass spheres is significantly affected by sliding and rolling frictions, particle size, and container thickness, but not density, Poisson's ratio, damping coefficient, or Young's modulus. The authors observed that the angle of repose increases with increasing rolling or sliding friction coefficients and with decreasing particle size or container thickness. However, container thickness larger than a critical value (about a 20-particle diameter) gives a constant angle of repose corresponding to a situation without any wall effects. This was shown by simulation results with periodic boundaries applied to opposite walls of the container. Periodic boundary conditions enable any particle leaving the domain in that direction to instantly re-enter on the opposite side (DEM Solutions, 2009), simulating infinite length in that direction and, thereby eliminating wall friction. In addition, the effect of particle size was mainly the result of its effect on rolling friction and not on sliding friction.

Measured angles of repose of grains and oilseeds for filling or piling and for emptying or funneling were found in the literature (Table 1).

Modeling with DEM

A review of the literature found the physical properties for soybean, corn, wheat, grain sorghum, rice, barley, oat, sunflower, and canola seeds listed in Table 1. Table 2 lists the moisture-dependent characteristics of soybeans and Table 3 is a summary of published and representative values of material and interaction properties of soybeans. Selected representative values of material properties (i.e., particle density, particle Poisson's ratio, and particle shear modulus) and interaction properties (i.e., particle coefficient of restitution and particle coefficient of static friction) were used as base values, which are used as inputs to DEM modeling. DEM modeling software used was EDEM 2.1.2 (DEM Solutions, Lebanon, N.H.). A range of each of these five physical properties was investigated in DEM simulations of basic physical property tests, using four particle shapes.

DEM is a numerical modeling technique that simulates dynamic motion and mechanical interactions of each particle using Newton's Second Law of Motion and force-displacement law. In DEM modeling, particle interactions are treated as a dynamic process, which assumes that equilibrium states develop whenever internal forces in the system balance (Theuerkauf et al., 2007). Contact forces and displacements of a stressed particle assembly are found by tracking the movement of individual particles. Newton's Law of Motion gives the relationship between particle motion and the forces acting on each particle. Particles interact only at contact points with their motion independent of the other particles. The soft-sphere approach commonly used in DEM models allows the particles to overlap each other giving realistic contact areas. Overlaps of the particles are allowed, but are small in comparison to the particle size. Force-displacement laws at the contacts are based on Hertzian contact theory (Mindlin, 1949; Mindlin and Deresiewicz, 1953; Tsuji et al., 1992; Di Renzo and Di Maio, 2004, 2005). Normal and tangential forces, velocities, and related parameters are described by appropriate equations from mechanics of particles (Tsuji et al., 1992; DEM Solutions, 1009; Remy et al., 2009).

In this study, DEM simulations were conducted with varying physical properties of soybean kernels, based on values in the literature, to find property combinations that gave simulation results that correlate well with measured bulk properties of soybeans while maintaining or improving computational speed. Thus, an appropriate particle model was established for DEM simulations of soybean handling operations. The following input parameters were included: (1) coefficient of restitution, (2) particle coefficient of static friction, (3) particle coefficient of rolling friction, (4) particle size distribution (PSD), (5) particle shear modulus, and (6) particle shape (i.e., from one to four overlapping spheres). Table 4 lists the variations in input parameters and includes test combination codes for the parameters: (1^{st} digit) particle coefficient of restitution, (2nd digit) particle coefficient of static friction, (3rd digit) particle coefficient of rolling friction, (4th digit) particle size distribution (PSD), and (5th digit) particle shear modulus.

The base value (represented by 1 in the test combination codes) of the particle coefficient of restitution was 0.6, which is the mean of published values. The second (0.3) and third (0.9) values for coefficients of restitution were chosen as extreme values inclusive of the published range (from 0.5 to 0.7). The base value of the particle coefficient of static friction on soybean-soybean contact was 0.55. The coefficient of static friction for soybean-steel interaction was computed to be 67% of the base value for soybean-soybean contact from Stahl (1950) and Mohsenin (1986). For particle rolling friction, the base value assumed in the simulation was 0.1, which was twice that of Zhou et al.'s (2002) for coarse glass beads, since grain surface is rougher than that of glass beads. For PSD, fixed or uniform size distribution was used first as the base value; normal PSD with a standard deviation factor (SDF) of 0.2 was second; and normal PSD with SDF of 0.4 was third. SDF was obtained from the coefficient of variation of single-kernel mass from 10 soybean lots (Table 5). The base value for particle shear modulus was the mean of the published values (41.7 MPa). Typically, shear modulus values do not greatly affect results, but smaller values of shear modulus are known to reduce computational time (Chung and Ooi, 2008; Remy et al., 2009); thus, the variation of shear modulus was towards lower values. The second value chosen was the lowest limit of the range of published shear modulus for soybeans (13.8 MPa). The very low third value (1.04 MPa), computed from Remy et al.'s (2009) particle Young's modulus (2.6 MPa) and the base value of the particle Poisson's ratio for soybeans (0.25), was selected for the potential to significantly reduce computation times. Table 6 shows the test combinations of the five parameters used with the 1-sphere particle shape. Simulations using test combination 11111 were performed with the 2-, 3-, and 4-sphere particle shapes.

Particle Shape

Four particle shapes were evaluated to represent soybean kernels (Figure 1). Particle shape was defined using one to four overlapping spheres. Geometry and dimension (length, width, and thickness) of the 4-sphere model were based on the soybean model of LoCurto et al. (1997) and Vu-Quoc et al. (2000), with slight differences in dimension to fit soybeans' published base values for particle density and particle volume (Table 3). Table 7 shows basic physical properties of the four particle shapes and positions of their spheres employed in the simulation. The position of each sphere in the x-, y-, and z-direction composing a particle shape is needed to define the particle shape in the simulation. Positions of the 1-, 2-, and 3-sphere particle shapes were modified to match the volume and particle density of the 4-sphere particle shape.

Accuracy tests for the particle coefficient of restitution was performed for all test combinations by simulating the dropping of 50 soybean particles from a height of 151 mm on a flat steel surface. The height was based on the drop tests of LoCurto et al.(1997) for soybeans. Drop and rebound heights were extracted from the simulation only from those particles with rebound trajectories that were vertical, based on LoCurto et al.'s (1997) criteria. The simulated rebound heights were used to calculate particle restitution coefficients. The calculated restitution coefficients were compared to the input restitution coefficients, which gave an indication of the simulation accuracy.

Table 2. Moisture-dependent properties of soybean kernels.

Parameters		Moisture Content (% wb)													
		6.9	7.0	7.1	8.0	8.1	9.7	9.8	10.0	10.7	12.2	13.0	13.4	15.5	16.7
Particle Length (mm), *l*					8.2 [F]		7.3 [E]		7.0 [D]				7.1 [D]		7.3 [D]
Particle Width (mm), w					6.6 [F]		6.1 [E]		6.6 [D]				6.6 [D]		6.7 [D]
Particle Thickness (mm), *h*					5.6 [F]		5.5 [E]		5.7 [D]				5.7 [D]		5.9 [D]
Particle Equivalent Diameter (mm), d_e															
Particle Radius (mm), r_e															
Particle Mass (mg), m					185.0 [F]		149.0 [E]		167.6 [D]				173.9 [D]		189.5 [D]
Particle Volume (mm^3), V									134.1 [D]				139.1 [D]		152.8 [D]
Particle Density (kg/m^3), ρ_p		1180 [G]	1130 [G]		1325.2 [F]				1250 [D]				1250 [D]		1243 [D]
Bulk Density (kg/m^3), ρ_b					739 ± 3 [F]				723 [D]	876 [C]			712 [D]	850 [C]	705 [D]
Particle Poisson Ratio, v					0.15 ± 0.02 [F]		0.4134 [E]		0.4 [A]			0.4 [A]			
Particle Elastic Modulus (MPa), E					32.6 ± 1.4 [F]		128.8 [E]		176.9 [A]			112.7 [A]			
Particle Shear Modulus (MPa), $G = E / (2 + 2v)$					13.33 - 15.04 [F]		45.56 [E]		63.18 [A]			40.25 [A]			
Particle Restitution Coefficient	with aluminum									0.7 [C]				0.6 [C]	
Particle Static Friction Coefficient	with galvanized sheet metal			0.21 [B]	0.23 - 0.27 [F]	0.21 [B]		0.18 [B]			0.20 [B]				
	with stainless steel				0.223 - 0.247 [F]										
Bulk Static Angle of Repose (deg)	for emptying or funneling				32.5 ± 0.5 [F]										
Bulk Angle of Internal Friction (deg)					30.1 ± 0.9 [F]										

[A] Misra and Young (1981)
[B] Mohsenin (1986, p. 801); Brubaker and Pos (1965)
[C] LoCurto et al. (1997)
[D] Nelson (2002)
[E] Zhang and Vu-Quoc (2002)
[F] Molenda and Horabik (2005)
[G] ASABE Standards (2006a) - D241.4

Table 3. Published properties of soybeans and their selected representative values.[a]

Parameters		Soybean Range		Representative Value	
Moisture Content (%) wb		6.9 - 16.7	B, D, E, F, I, J, L, M		
Particle Length (mm), *l*		7.0 - 8.2	G, I, J, L	7.6	G, I, J, L
Particle Width (mm), w		6.1 - 6.7	G, I, J, L	6.4	G, I, J, L
Particle Thickness (mm), *h*		5.5 - 5.9	G, I, J, L	5.7	G, I, J, L
Particle Equivalent Diameter (mm), d_e		6	E, K	6	E, K
Particle Radius (mm), r_e		3	E, K	3	E, K
Particle Mass (mg), *m*		100 - 200	G, H, I, J, L	150	G, H, I, J, L
Particle Volume (mm^3), *V*		134.1 - 152.8	I	143.5	I
Particle Density ($kg \cdot m^{-3}$), ρ_p		1130.0 - 1325.2	I, K, L, M	**1228**	I, K, L, M
Bulk Density ($kg \cdot m^{-3}$), ρ_b		705.0 - 876.0	C, F, I, L, M	790.5	C, F, I, L, M
Particle Poisson Ratio, *v*		0.08 - 0.4134	D, G, J, K, L	**0.25**	D, G, J, K, L
Particle Elastic Modulus (MPa), *E*		31.2 - 176.9	D, J, K, L	104.1	D, J, K, L
Particle Shear Modulus (MPa), $G = E / (2 + 2v)$		13.8 - 63.2	D, J, K, L	**41.7**	D, J, K, L
Particle Restitution Coefficient, *e*	with self (grain)	-		**0.60**	F, G, K
	generic	0.5, 0.7	K, G		
	with aluminum	0.6, 0.7	F		
	with steel	-		**0.60**	F, G, K
Particle Static Friction Coefficient, μ_s	with self (grain)	0.267, 0.55	A, E, G	**0.55**	A, E
	with galvanized sheet metal	0.18 - 0.27	B, E, L		
	with steel	0.223 - 0.247, 0.37	A, E, L	**0.37**	A, E
	with transparent perspex	0.30	K		
	with glass	0.328	G		
Particle Rolling Friction Coefficient	with self (grain)	-		**0.10**	assume
	with steel	-		**0.10**	assume
Bulk Static Angle of Repose (degree)	for filling or piling	16	A, E	16	A, E
	for emptying or funneling	29 - 33	A, E, L	31	A, E, L
Bulk Angle of Internal Friction (degree)		29.2 - 31	L	30	L

[a] Representative values in bold letters were used as base values in simulation.

A Stahl (1950)
B Brubaker and Pos (1965)
C Henderson and Perry (1976)
D Misra and Young (1981)
E Mohsenin (1986)
F LoCurto et al. (1997)
G Vu-Quoc et al. (2000)
H McLelland and Miller (2001)
I Nelson (2002)
J Zhang and Vu-Quoc (2002)
K Raji and Favier (2004a, 2004b)
L Molenda and Horabik (2005)
M ASAE Standards (2006a) - D241.4

Table 4. Variation of input parameters.

Parameter	Symbol	Base Value (1)	Second Value (2)	Third Value (3)
1. Particle Restitution Coefficient	e	0.60	0.30	0.90
2. Particle Static Friction Coefficient				
(soybean-soybean)	$\mu_{s\ (so\text{-}so)}$	0.55	0.35	0.75
(soybean-steel)	$\mu_{s\ (so\text{-}st)}$	0.37	0.23	0.50
3. Particle Rolling Friction Coefficient	μ_r	0.10	0.05	0.20
(soybean-soybean is assumed same as soybean-steel)				
4. Particle Size Distribution	*PSD*	fixed or uniform	normal	normal
Mean factor	*MF*	1.0	1.0	1.0
Standard deviation factor	*SDF*	0.0	0.20	0.40
5. Particle Shear Modulus (MPa)	*G*	41.7	13.8	1.04

Table 5. Experimental data for standard deviation factor (SDF) for particle size distribution.[a]

						Single Kernel Mass, mg		
No.	**Variety**	**Source**	**Location Planted**	**Crop Year**	**No. of Kernels Weighed**	**Mean**	**Standard Deviation (SD)**	**Coefficient of Variation (CV), %**
1	9A411NRR	Kaufman Seeds	Reno County, Kansas	2008	55	144.24	25.41	17.62
2	9A385NRS	Kaufman Seeds	Reno County, Kansas	2007	50	112.85	20.14	17.85
3	KS-5005sp	KSU Agronomy Farm	Riley County, Kansas	2007	51	221.40	40.00	18.06
4	KS-3406RR	KSU Agronomy Farm	Riley County, Kansas	2007	55	132.97	26.14	19.66
5	KS-4607	KSU Agronomy Farm	Riley County, Kansas	2007	51	157.34	31.16	19.80
6	KS-4702sp	KSU Agronomy Farm	Riley County, Kansas	2007	56	122.64	26.12	21.29
7	Mixed (100-lb)	Manhattan Farmers COOP	Northeastern Kansas	2007	53	149.48	32.07	21.46
8	Mixed (7080-lb)	Manhattan Farmers COOP	Northeastern Kansas	2007	53	149.91	32.35	21.58
9	KS-5002N (4RL9542)	KSU Agronomy Farm	Riley County, Kansas	2004	55	157.42	34.39	21.84
10	KS-4103sp (4RL4976)	KSU Agronomy Farm	Riley County, Kansas	2004	56	124.19	28.46	22.91
				Mean	**53.50**	**147.24**	**29.62**	**20.21**
				SD	**2.22**	**30.27**	**5.57**	**1.88**

[a] SDF value of 0.2 was taken from the mean CV of individually weighing soybean kernels.

Table 6. Test combinations of input parameters. [a]

Test No.	Test Combinations				
	Particle Restitution Coefficient	Particle Static Friction Coefficient	Particle Rolling Friction Coefficient	Particle Size Distribution	Particle Shear Modulus
1-sphere					
1	1	1	1	1	1
2	2	1	1	1	1
3	3	1	1	1	1
4	1	2	1	1	1
5	1	3	1	1	1
6	1	1	2	1	1
7	1	1	3	1	1
8	1	1	1	2	1
9	1	1	1	3	1
10	1	1	1	1	2
11	1	1	1	1	3
2-sphere					
12	1	1	1	1	1
3-sphere					
13	1	1	1	1	1
4-sphere					
14	1	1	1	1	1

[a] Refer to Table 4 for complete interpretation.
Coefficient of restitution (1 stands for e = 0.6, 2 for e = 0.3, 3 for e = 0.9).
Coefficient of static friction (1 for $\mu_{s(so\text{-}so)}$ = 0.55, $\mu_{s(so\text{-}st)}$ = 0.37; 2 for $\mu_{s(so\text{-}so)}$ = 0.35, $\mu_{s(so\text{-}st)}$ = 0.23; 3 for $\mu_{s(so\text{-}so)}$ = 0.75, $\mu_{s(so\text{-}st)}$ = 0.50).
Coefficient of rolling friction (1 for μ_r = 0.1, 2 for μ_r = 0.05, 3 for μ_r = 0.2).
Particle size distribution (PSD) (1 for uniform particle size, 2 for normal PSD with standard deviation factor (SDF) = 0.2, 3 for normal PSD with SDF = 0.4).
Shear modulus (1 stands for G = 41.7 MPa, 2 for G = 13.8 MPa, 3 for G = 1.04 MPa).

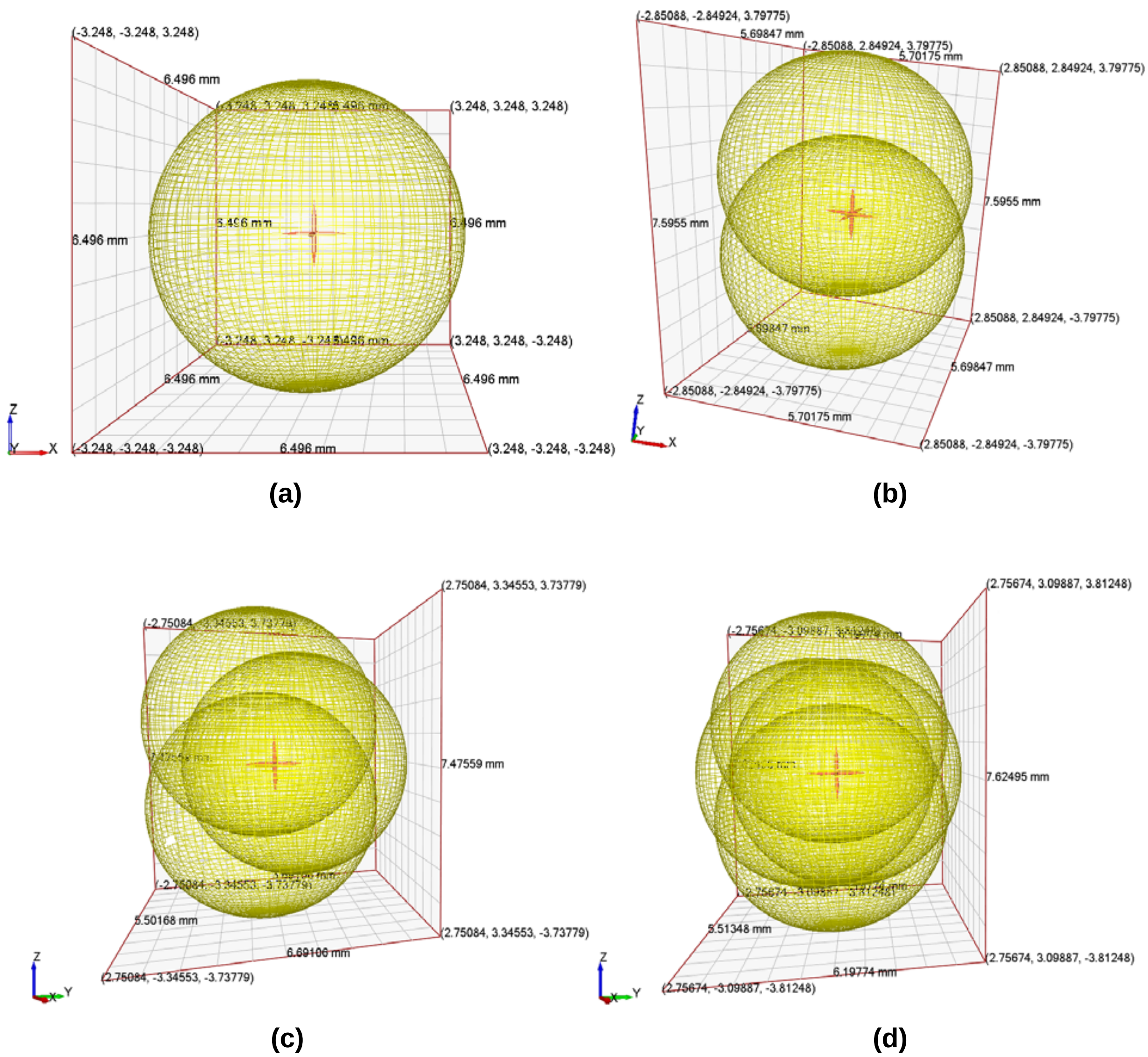

Figure 1. Particle shapes of soybean in the simulation: (a) 1-sphere model; (b) 2-sphere model; (c) 3-sphere model; and (d) 4-sphere model (drawn in EDEM Academic software).

Table 7. Properties of the four particle models and positions (x, y, z) of each sphere in EDEM.

Parameter		Particle shape			
		1-Sphere	2-Sphere	3-Sphere	4-Sphere
Length of soybean (mm)	l_b	6.496	7.59550	7.47559	7.62495
Width of soybean (mm)	w_b	6.496	5.70175	6.69106	6.19774
Height of soybean (mm)	h_b	6.496	5.69847	5.50168	5.51348
Radius of sphere (mm)	R	3.248	2.85	2.75	2.75
Volume (m^3)	V_b	1.4350E-07	1.4350E-07	1.4350E-07	1.4350E-07
Mass (kg)	m_b	0.0001763	0.0001762	0.0001762	0.0001762
Particle Density ($kg \cdot m^{-3}$)	ρ_b	1228.0	1228.0	1228.0	1228.0
Position		**Particle shape**			
		1-Sphere	**2-Sphere**	**3-Sphere**	**4-Sphere**
Surface 1 (X, Y, Z)		(0, 0, 0)	(0, 0, 0)	(0, 0, 0)	(0, -0.35, 0)
Surface 2 (X, Y, Z)		-	(0, 0, 1.89)	(0, 0, 1.975)	(0, 0.35, 0)
Surface 3 (X, Y, Z)		-	-	(0, 0.8, 0.9875)	(0, 0, 1.062)
Surface 4 (X, Y, Z)		-	-	-	(0, 0, -1.062)

Bulk Density Test

The bulk density test was based on USDA GIPSA's (2004) procedure for test-weight-per-bushel apparatus (Figure 2). Dimensions of the inside diameter and height of the kettle were 117.475 mm (4.625 in.) and 101.60 mm (4.0 in.), respectively. The test-weight kettle was drawn in a computer-aided design (CAD) software (DS SolidWorks Corp., Concord, Mass.) and imported to establish model geometries in the simulation software. The hopper above the kettle was also drawn with the standard 31.75-mm (1.25 in.) opening and a standard distance from the kettle of 50.8 mm (2.0 in.) (USDA-GIPDA, 1996).

Particles coming from the hopper dropped to fill the kettle. Excess particles were allowed to overflow. Simulation time for each test combination was between 20 to 120 s, depending on the time the kettle was filled and the particles stopped flowing. Simulation time was determined by the particles stabilizing on top of the kettle and the kinetic energy of the whole system approaching zero.

To get the bulk density (ρ_b) in $kg \cdot m^{-3}$, only the total mass of particles filling the kettle (m_p) in kg was computed from the simulation. The mass of piled particles on top and outside of the kettle was excluded in the calculation. The computed mass of particles inside the kettle was divided by the volume of the kettle (V_k) in m^3 (Equation 4). The mean bulk density for three replications for each test combination was computed.

$$\rho_b = \frac{m_p}{V_k} \qquad (4)$$

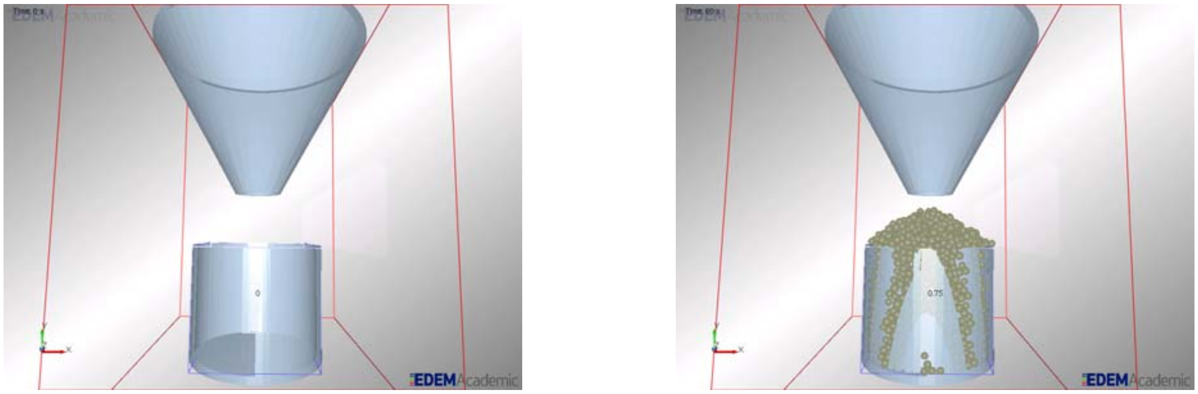

(a) (b)

Figure 2. Bulk density tests in simulation: (a) empty test-weight (TW) kettle and (b) full TW kettle.

Bulk Angle of Repose Test

The tilting box method was employed to simulate the angle of repose test of soybean particles in DEM (Figure 3). A box measuring 240 x 120 x 40 mm was drawn and filled with soybean particles in the simulation. Train (1958) recommended that the width of the box be at least one-third of its length to reduce wall effects. In this simulation, the width was one-half of the length, which satisfied Train's (1958) recommendation.

Moreover, periodic boundaries were used on opposite sides of the simulation box (in the direction of the width = 120 mm). Periodic boundary conditions enable any particle leaving the domain in that direction to instantly re-enter on the opposite side, simulating infinite length in that direction and, thereby eliminating wall friction. Base friction was also removed by ensuring the base of the box had the same frictional coefficients as that of the particles.

After 0.15 s of filling the box up to the rim, the box was then tilted at a constant angular velocity of 90 $deg \cdot s^{-1}$ until particles begin to move, and then the simulation was stopped after 0.65 to 0.85 s depending on the test combinations being evaluated. The time when the particles began to move was recorded, which allowed calculation of the angle of repose of the soybeans based on the angular velocity of the tilting box. Both the actual particle motions and the vectors of the particle motions were evaluated to determine the start of particle movement. The mean angle of repose for seven replications for each test combination was calculated.

Data Analysis

Statistical analysis of results was performed using the generalized linear model (GLM) procedure of SAS statistical software (version 9.2, SAS Institute, Inc., Cary, NC). Mean, standard deviation, and percentage difference from expected input and published values were determined from the coefficient of restitution, angle of repose, and bulk density tests. The simulation results were compared with the literature values based on their percentage differences. Differences among test combinations within the coefficient of restitution, angle of repose, and bulk density tests were compared using the Bonferroni Multiple Comparison Test in SAS at the 5% level of significance. Bonferroni uses strict requirements prior to rejecting the null hypotheses, which minimizes Type I errors. Test combinations having simulation results best correlating with the literature values were chosen to simulate soybeans in ongoing simulations of grain commingling.

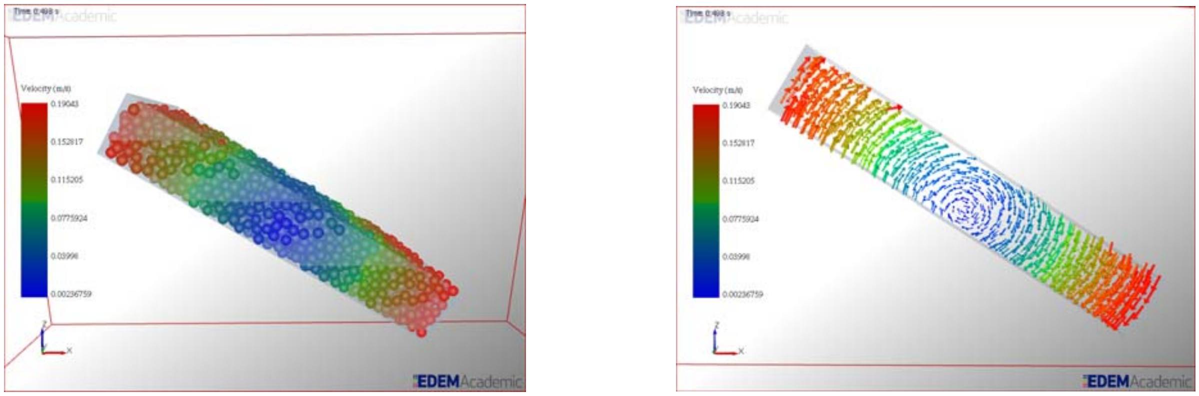

(a) **(b)**

Figure 3. Angle of repose test in simulation: (a) particle mode and (b) vector mode.

Results and Discussion

In choosing the best particle model for soybeans, tradeoffs between the two criteria, namely bulk density and angle of repose, were required. The particle model was also revised by combining and refining input parameters that performed well in the two tests.

In the accuracy tests, the input parameter was the particle coefficient of restitution and the output calculated from the rebound height had the same particle restitution values. All test combinations with the base particle restitution value of 0.6 had percent deviations ranging from 0.68% to 1.77% and were not significantly different ($p > 0.05$) from each other. When the restitution coefficient was varied (cases 21111 and 31111), the percent deviation from the input value ranged from 0.25% to 7.6%. The 0.25% deviation was obtained from the test combination with the highest particle restitution value (0.9) and the 7.6% deviation was from that with the lowest particle restitution (0.3). Thus, only artificially low values of the restitution coefficient caused excessive accuracy issues, and these low values were not pursued further for the particle models.

Bulk Density Test

Bulk density increased with the coefficient of restitution but decreased with coefficients of static and rolling friction (Table 8). Wider size distributions increased bulk density as observed from test combinations 11121 to 11131. This may be explained by the increasing standard deviation factor (from 0.2 to 0.4) in the particle size distribution, which increases the smaller particles in the normal size distribution. These small particles were filling the void in between large particles, thereby increasing the bulk density.

Simulations involved fixed particle size within each particle shape. Particle density and mass were constant among particle shapes. Results showed that bulk density decreased as the number of spheres in a particle shape increased, except for the case of 1-sphere particle shape. This can be explained by a 4-sphere particle shape occupying a slightly higher volume than a 2-sphere particle shape, thus, slightly decreasing the bulk density. Bulk densities from 2- to 4-sphere particle shapes, however, were not significantly different ($p > 0.05$) from each other. Bulk densities of the 1- and 4-sphere particle shapes were also not significantly different ($p > 0.05$).

In general, the simulations resulted in lower bulk densities than the published values. Test combinations 31111, 12111, 11211, 11131, and 11113 for 1-sphere particle shape and 11111 for 2-sphere particle shape gave bulk densities closer to the literature value of 720.72 $kg \cdot m^{-3}$. Test combination 31111 was significantly different ($p < 0.05$) from all other test combinations. Test combinations 12111, 11211, and 11113 were significantly different ($p < 0.05$) from 11131 for the 1-sphere particle shape, but did not differ ($p > 0.05$) from test combination 11111 for the 2-sphere particle shape.

Table 8. Results of bulk density and bulk angle of repose tests for initial test combinations.[a]

	Bulk Density, $kg \cdot m^{-3}$				Bulk Angle of Repose, deg.			
Combination No.	**Simulation Value**		**Published Value**	**% Diff**	**Simulation Value**		**Published Value**	**% Diff**
1st Iteration								
Restitution								
1s_11111 (e=0.6)	669.00 a h	(1.60)	720.72	-7.18	31.50 a e	(0.35)	31.0	1.61
1s_21111 (e=0.3)	660.39 b	(0.77)	720.72	-8.37	32.31 a	(0.82)	31.0	4.23
1s_31111 (e=0.9)	687.12 c	(0.93)	720.72	-4.66	37.17 b	(0.47)	31.0	19.91
Static Friction								
1s_11111 (μ_s=0.55)	669.00 a h	(1.60)	720.72	-7.18	31.50 a e	(0.35)	31.0	1.61
1s_12111 (μ_s=0.35)	678.30 d g	(2.00)	720.72	-5.89	31.50 a e	(1.25)	31.0	1.62
1s_13111 (μ_s=0.75)	665.67 a	(3.03)	720.72	-7.64	37.35 b	(1.47)	31.0	20.49
Rolling Friction								
1s_11111 (μ_r=0.1)	669.00 a h	(1.60)	720.72	-7.18	31.50 a e	(0.35)	31.0	1.61
1s_11211 (μ_r=0.05)	680.08 d	(0.33)	720.72	-5.64	30.52 c e	(0.50)	31.0	-1.54
1s_11311 (μ_r=0.2)	656.61 b	(0.72)	720.72	-8.89	35.28 d	(0.98)	31.0	13.81
Size Distribution								
1s_11111 (SDF=0)	669.00 a h	(1.60)	720.72	-7.18	31.50 a e	(0.35)	31.0	1.61
1s_11121 (SDF=0.2)	668.51 a h	(0.28)	720.72	-7.24	29.30 c	(0.48)	31.0	-5.48
1s_11131 (SDF=0.4)	670.60 e h	(2.89)	720.72	-6.95	32.64 a	(1.10)	31.0	5.31
Shear Modulus								
1s_11111 (G=41.7MPa)	669.00 a h	(1.60)	720.72	-7.18	31.50 a e	(0.35)	31.0	1.61
1s_11112 (G=13.8 MPa)	671.44 e f h	(2.25)	720.72	-6.84	31.45 a e	(0.50)	31.0	1.45
1s_11113 (G=1.04 MPa)	679.93 d	(0.28)	720.72	-5.66	32.75 a	(0.66)	31.0	5.65
Particle Model								
1s_11111	669.00 a h	(1.60)	720.72	-7.18	31.50 a e	(0.35)	31.0	1.61
2s_11111	675.55 d g f	(0.95)	720.72	-6.27	29.28 c	(0.29)	31.0	-5.56
3s_11111	673.89 e f g	(1.05)	720.72	-6.50	29.12 c	(0.55)	31.0	-6.06
4s_11111	672.53 e f h	(0.59)	720.72	-6.69	29.42 c	(1.18)	31.0	-5.10

[a] Mean values with the same lower case letters within a column are not significantly different at the 5% level of significance in Bonferroni. Values in parentheses represent standard deviation (SD).
Particle shape (1s = 1-sphere; 2s = 2-sphere; 3s = 3-sphere; 4s = 4-sphere).
Coefficient of restitution (1 stands for e = 0.6; 2 for e = 0.3; 3 for e = 0.9).
Coefficient of static friction (1 for $\mu_{s(so\text{-}so)}$ = 0.55, $\mu_{s(so\text{-}st)}$ = 0.37; 2 for $\mu_{s(so\text{-}so)}$ = 0.35, $\mu_{s(so\text{-}st)}$ = 0.23; 3 for $\mu_{s(so\text{-}so)}$ = 0.75, $\mu_{s(so\text{-}st)}$ = 0.50).
Coefficient of rolling friction (1 for μ_r = 0.1; 2 for μ_r = 0.05; 3 for μ_r = 0.2).
Particle size distribution (PSD) (1 for uniform particle size; 2 for normal PSD with standard deviation factor (SDF) = 0.2; 3 for normal PSD with SDF = 0.4).
Shear modulus (1 stands for G = 41.7 MPa, 2 for G = 13.8 MPa, 3 for G = 1.04 MPa).

Bulk Angle of Repose Test

Static and rolling friction coefficients affect the angle of repose. In general, as the static and rolling friction coefficients increased so did the angle of repose in the simulation (Table 8). This observation was similar to that of Zhou et al. (2002) and Walton (1994).

The greater the number of spheres in a particle model, the higher the angle of repose. Walton and Braun (1993) and Walton (1994) found increasing values of dynamic angle of repose as spheres increased from mono to cubic (8-sphere). Simulation results of static angle of repose, however, did not exactly agree with those authors' findings. This was likely due to the volume of the particle models always being the same during simulation so particles did not increase in size as the number of spheres in a particle model increased, unlike the previous authors observed. The 1-sphere particle shape showed a very high angle of repose, whereas the 3-sphere particle shape gave the lowest angle. The 4-sphere particle shape had a higher angle of repose than the 2-sphere shape, which agreed with the published trend of Walton's group.

Angle of repose increased for wider size distribution (i.e., from PSD with SDF = 0.2 to that with SDF = 0.4). This result for static angle agreed with Zenz's (1957) experimental findings for dynamic angle of repose.

For 1-sphere particle models, test combinations 11111, 12111, 11211, 11131, and 11112 gave closer values to the published angle of repose (31°) and were not significantly different ($p > 0.05$) from each other.

For multi-sphere particle models, results of test combination 11111 for the 4-sphere shape were closest to the published angles of repose. This test combination, however, did not significantly differ ($p > 0.05$) from test combination 11111 for 2- and 3-sphere shapes.

Best-Correlated Particle Models

In general, multi-sphere particle shapes did not give promising results in the bulk property tests. During initial testing (Table 8), combination 31111 with the highest particle coefficient of restitution (0.9) resulted in the closest bulk density (687.12 $kg \cdot m^{-3}$) to published values (720.72 $kg \cdot m^{-3}$). The angle of repose of the bulk materials from this test combination (37.17°), however, was higher than the literature value (31°). The high bulk density and angle of repose may be explained by the high coefficient of restitution of the particle in the parameter mix of that test combination. In a second iteration, modified testing was performed to determine whether lowering the particle restitution (to 0.7 or 0.8) would result in a more desirable bulk angle of repose, yet still maintain bulk density close to the expected value. Bulk density tests, including coefficients of restitution of 0.7 (test combination 4111) and 0.8 (test combination 5111), resulted in values of 671.77 and 679.45 $kg \cdot m^{-3}$, respectively (Table 9). These values, however, were lower than the bulk density values of test combinations 11211 (680.08 $kg \cdot m^{-3}$) and 11113 (679.93 $kg \cdot m^{-3}$) from the initial testing (Table 8); thus, they were not tested for angle of repose. For bulk angle of repose, test combinations 11112 (31.45°) and 11211 (30.52°) yielded values closest to the published one with percent deviations of 1.45% and -1.54%, respectively.

Table 9. Results of bulk density and bulk angle of repose tests for possible best test combination.

Combination No.		Bulk Density, kg·m^{-3} Simulation Value		Expected Value	% Diff	Angle of Repose, deg. Simulation Value		Expected Value	% Diff
2nd Iteration									
1s_12233	(μ_s=0.35)	697.90 a	(1.76)	720.7	-3.17	28.54 a	(0.58)	31.0	-7.94
1s_11231	(μ_s=0.55, G=41.7MPa)	682.37 b	(1.50)	720.7	-5.32	31.54 b	(0.53)	31.0	1.74
1s_11232	(μ_s=0.55, G=13.8MPa)	682.47 b	(1.58)	720.7	-5.31	32.15 b c	(0.72)	31.0	3.70
1s_11233	(μ_s=0.55, G=1.04MPa)	685.09 b c	(5.65)	720.7	-4.94	31.90 b	(0.68)	31.0	2.90
1s_14231	(μ_s=0.58, G=41.7MPa)	680.74 b	(1.64)	720.7	-5.55	33.14 c d	(0.40)	31.0	6.90
1s_14232	(μ_s=0.58, G=13.8MPa)	681.77 b	(1.27)	720.7	-5.40	31.03 b	(0.48)	31.0	0.11
1s_14233	(μ_s=0.58, G=1.04MPa)	690.47 c	(0.60)	720.7	-4.20	33.45 d	(1.01)	31.0	7.90
1s_41111	(e=0.7)	671.77 d	(1.36)	720.7	-6.79				
1s_51111	(e=0.8)	679.45 b	(0.68)	720.7	-5.73				
3rd Iteration									
1s_12233	(μ_s=0.35)	697.90 a	(1.76)	720.7	-3.17	28.54 a	(0.58)	31.0	-7.94
1s_17233	(μ_s=0.40)	695.39 a	(0.83)	720.7	-3.51	29.01 a	(0.36)	31.0	-6.42
1s_16233	(μ_s=0.45)	693.73 a	(1.15)	720.7	-3.74	30.89 b	(0.53)	31.0	-0.36
1s_15233	(μ_s=0.50)	693.58 a	(1.82)	720.7	-3.77	31.20 b	(0.45)	31.0	0.66
1s_11233	(μ_s=0.55)	685.09 b	(5.65)	720.7	-4.94	31.90 b	(0.68)	31.0	2.90
1s_14233	(μ_s=0.58)	690.47 a b	(0.60)	720.7	-4.20	33.45 c	(1.01)	31.0	7.90

[a] Mean values with the same lower case letters within a column are not significantly different at the 5% level of significance in Bonferroni. Values in parentheses represent standard deviation (SD).
Particle shape (1s = 1-sphere).
Coefficient of restitution (1 stands for e = 0.6; 4 for e = 0.7; 5 for e = 0.8).
Coefficient of static friction (1 for $\mu_{s(so\text{-}so)}$ = 0.55, $\mu_{s(so\text{-}st)}$ = 0.37; 2 for $\mu_{s(so\text{-}so)}$ = 0.35, $\mu_{s(so\text{-}st)}$ = 0.23; 4 for $\mu_{s(so\text{-}so)}$ = 0.58, $\mu_{s(so\text{-}st)}$ = 0.39; 5 for $\mu_{s(so\text{-}so)}$ = 0.50, $\mu_{s(so\text{-}st)}$ = 0.34; 6 for $\mu_{s(so\text{-}so)}$ = 0.45, $\mu_{s(so\text{-}st)}$ = 0.30; 7 for $\mu_{s(so\text{-}so)}$ = 0.40, $\mu_{s(so\text{-}st)}$ = 0.27).
Coefficient of rolling friction (1 for μ_r = 0.1; 2 for μ_r = 0.05).
Particle size distribution (PSD) (1 for uniform particle size; 3 for normal PSD with SDF = 0.4).
Shear modulus (1 stands for G = 41.7 MPa, 2 for G = 13.8 MPa, 3 for G = 1.04 MPa).

With tradeoffs between bulk density and bulk angle of repose, test combination 11211 gave the best correlated coefficients of restitution, static friction, and rolling friction, which were 0.6, 0.55 (for soybean-soybean; 0.37 for soybean-steel), and 0.05, respectively (Table 8). However, test combination 11211 did not include size distribution of the particles because it only represented uniform or fixed particle sizes. Thus, the normal PSD with SDF of 0.4 was chosen because test combination 11131 performed better in the bulk density and bulk angle of repose tests than 11121. For particle shear modulus, test combination 11113 (G = 1.04 MPa) did better in the bulk density test while test combination 11112 (G = 13.8 MPa), did best in the angle of repose test (Table 8). Both particle shear moduli were included in the second iteration, together with the highest shear modulus (G = 41.7 MPa), to determine how these shear moduli performed when combined with the other parameters (i.e., coefficients of restitution, rolling and static friction, and PSD). The second iteration also included the second particle coefficient of static friction of 0.35 (for soybean-soybean; 0.23 for soybean-steel), which was in 12111 due to the test combination's bulk density being higher than that of 11112.

In the second iteration, test combinations 12233 and 14233, with particle static friction of 0.35 and 0.58, respectively, produced the best values for bulk density. The bulk angles of repose results, however, were poor for those combinations (Table 9).

A third iteration was performed using test combinations with particle static friction between 0.35 and 0.58. This iteration determined which particle static friction would give the highest bulk density while maintaining the best possible value for bulk angle of repose. The third iteration revealed that the best parameter mix was test combination 16233, which included particle coefficients of restitution static friction for soybean-soybean (soybean-steel) and rolling friction of 0.6, 0.45 (0.30), and 0.05, respectively; PSD with SDF of 0.4; and particle shear modulus of 1.04 MPa (Table 9). In addition, test combination 16233 made the computational time faster (Chung and Ooi, 2008; Remy et al., 2009) due to the low particle shear modulus (G=1.04MPa).

Summary and Conclusion

Material and interaction properties of various grains and oilseeds relevant to discrete element modeling (DEM) were reviewed. Material properties were particle shape and size, Poisson's ratio, shear modulus, and density. Interaction properties included coefficients of restitution, static friction, and rolling friction. Published values were used as base values for simulation modeling. Single- and multi-sphere soybean particle models, comprised of one to four overlapping spheres, were compared based on DEM simulations of the bulk properties: bulk density and angle of repose.

A particle model with a single sphere best simulated soybean kernels in the bulk property tests. The best particle model included a particle coefficient of restitution of 0.6, particle static friction of 0.45 for soybean-soybean contact (0.30 for soybean-steel interaction), particle rolling friction of 0.05, normal particle size distribution with a standard deviation factor of 0.4, and particle shear modulus of 1.04 MPa. To optimize the simulated bulk properties, most parameters in this particle model varied only a small amount from the base values obtained from the literature. However, the particle shear modulus was set artificially low since that helped speed up the simulations without negatively impacting the simulation of bulk properties. This particle model will be used to simulate soybeans in grain handling and enhance the prediction of grain commingling in bucket elevator equipment.

Acknowledgements

The research was supported by the U.S. Department of Agriculture (CRIS No. 5430-43440-005-00D). The technical advice of Dr. Oleh Baran (*DEM Solutions*), Dr. Christoph Hiemcke (*formerly with DEM Solutions*), Dr. Otis Walton (*Grainflow Dynamics, Inc.*), Dr. Ray Bucklin (*University of Florida*), and Dr. Jasper Tallada (*GMPRC*) is highly appreciated.

References

Airy, W. 1898. The pressure of grain. In *Minutes of Proceedings of the Institution of Civil Engineers*, vol. 131, 347-358. J. H. T. Tudsbery, ed. London: Institution of Civil Engineers.

Arnold, P. C. and A. W. Roberts. 1969. Fundamental aspects of load-deformation behavior of wheat grains. *Transactions of the ASAE* 12(1): 104-108.

ASAE Standards. 2006a. D241.4. Density, specific gravity, and mass-moisture relationships of grain for storage. St. Joseph, Mich.: ASAE.

ASAE Standards. 2006b. S368.4. Compression test of food materials of convex shape. St. Joseph, Mich.: ASAE.

Bardet, J. P. and Q. Huang. 1993. Rotational stiffness of cylindrical particle contacts. In *Powders and Grains 93*, 39-43. C. Thornton, ed. Rotterdam: Balkema.

Berruto, R. and D. E. Maier. 2001. Analyzing the receiving operation of different grain types in a single–pit country elevator. *Transactions of the ASAE* 44(3): 631–638.

Bilanski, W. K., B. Szot, I. Kushwaha, and A. Stepneiwski. 1994. Comparison of strength features of rape pods and seeds for varieties cultivated in various countries. *International Agrophysics* 8(4): 177-184.

Boyles, M., T. Peeper, and M. Stamm. 2006. Great Plains Canola Production Handbook. MF-2734. Manhattan, Kansas: Kansas State University Cooperative Extension Service.

Brown, R. L. and J. C. Richards. 1959. Exploratory study of the flow of granules through apertures. *Chemical Engineering Research and Design (Transactions of the Institution of Chemical Engineers)* 37a: 108-119.

Brubaker, J. E. and J. Pos. 1965. Determining static coefficient of friction of grains on structural surfaces. *Transactions of the ASAE* 8(1): 53-55.

Burmistrova, M. F., I. K. Komol'kova, N. V. Klemm, M. T. Panina, I. M. Polunochev, A. I. P'yankov, A. F. Sokolov, N. G. Tetyanko, V. M. Chaus, and E. G. Eglit. 1963. *Physicomechanical Properties of Agricultural Crops.* Translated from Russian and published for the National Science Foundation. Jerusalem: Israel Program for Scientific Translations, Ltd.

Calisir, S., T. Marakoglu, H. Ogut, and O. Ozturk. 2005. Physical properties of rapeseed (*Brassica napus oleifera* L.). *Journal of Food Engineering* 69(1): 61-66.

Chung, Y. C., J. Y. Ooi, and J. F. Favier. 2004. Measurement of mechanical properties of agricultural grains for DE models. In *17th ASCE Engineering Mechanics Conference*. Newark, Del.: American Society of Civil Engineers.

Chung, Y. C. and J. Y. Ooi. 2008. Influence of discrete element model parameters on bulk behavior of a granular solid under confined compression. *Particulate Science and Technology* 26(1):83-96.

DEM Solutions. 2009. *EDEM 2.1.2 User Guide*. Lebanon, N.H.: DEM Solutions (USA), Inc. 138p.

Di Renzo, A. and Di Maio, F. P. 2004. Comparison of contact-force models for the simulation of collisions in DEM-based granular flow codes. *Chemical Engineering Science* 59(3): 525-541.

Di Renzo, A. and Di Maio, F. P. 2005. An improved integral non-linear model for the contact of particles in distinct element simulations. *Chemical Engineering Science* 60(5): 1303-1312.

Fowler, R. T. and W. B. Chodziesner. 1959. The influence of variables upon the angle of friction of granular materials. *Chemical Engineering Science* 10: 157-162.

Fowler, R. T. and F. A. Wyatt. 1960. The effect of moisture content on the angle of repose of granular solids. *Australian Journal for Chemical Engineers* 1: 5-8.

Fraczek, J., A. Zlobecki, and J. Zemanek. 2007. Assessment of angle of repose of granular plant material using computer image analysis. *Journal of Food Engineering* 83(1): 17-22.

Greenlees, W. J. and S. C. Shouse. 2000. Estimating grain contamination from a combine. ASAE Paper No. MC00103. St. Joseph, Mich.: ASAE.

Gupta, R. K. and S. K. Das. 1997. Physical properties of sunflower seeds. *Journal of Agricultural Engineering Research* 66(1): 1-8.

Hanna, H. M., D. H. Jarboe, and G. R. Quick. 2006. Grain residuals and time requirements for combine cleaning. ASAE Paper No. 066082. St. Joseph, Mich.: ASAE.

Henderson, S. M. and R. L. Perry. 1976. *Agricultural Process Engineering*. 3rd. ed. Westport, Conn.: The AVI Publishing Company. 430p.

Herrman, T. J., S. Baker, and F. J. Fairchild. 2001. Characterization of receiving systems and operating performance of Kansas grain elevators during wheat harvest. *Applied Engineering in Agriculture* 17(1): 77–82.

Herrman, T. J., M. A. Boland, K. Agrawal, and S. R. Baker. 2002. Use of a simulation model to evaluate wheat segregation strategies for country elevators. *Applied Engineering in Agriculture* 18(1): 105–112.

Hirai, Y., M. D. Schrock, D. L. Oard, and T. J. Herrman. 2006. Delivery system of tracing caplets for wheat grain traceability. *Applied Engineering in Agriculture* 22(5): 747-750.

Horabik, J. and J. Lukaszuk. 2000. Measurement of internal friction angle of wheat grain using triaxial compression test. *Acta Agrophysica* 37: 39-49 (in Polish).

Hoseney, R. C. and J. M. Faubion. 1992. Chapter 1: Physical properties of cereal grains. In *Storage of Cereal Grains and Their Products*. 4th. ed. D. B. Sauer, ed. St. Paul, Minn.: American Association of Cereal Chemists, Inc.

Hurburgh, C. R., Jr. 1999. The GMO controversy and grain handling for 2000. Paper presented at the Iowa State University Integrated Crop Management Conference. Available at: http://www.exnet.iastate.edu/Pages/grain/gmo/99gmoy2k.pdf. Accessed 21 June 2006.

Ingles, M. E. A., M. E. Casada, and R. G. Maghirang. 2003. Handling effects on commingling and residual grain in an elevator. *Transactions of the ASAE* 46(6): 1625-1631.

Ingles, M. E. A., M. E. Casada, R. G. Maghirang, T. J. Herrman, and J. P. Harner III. 2006. Effects of grain-receiving system on commingling in a country elevator. *Applied Engineering in Agriculture* 22(5): 713-721.

Jamieson, J. A. 1903. Grain pressures in deep bins. *Transactions of the Canadian Society of Civil Engineers* 17(2): 554-607.

Jiang, M. J., H. S. Yu, and D. Harris. 2005. A novel discrete model for granular material incorporating rolling resistance. *Computers and Geotechnics* 32(5): 340-357.

Kramer, H. A. 1944. Factors influencing the design of bulk storage bins for rough rice. *Agricultural Engineering* 25(12): 463-466.

Li, Y., Y. Xu, and C. Thornton. 2005. A comparison of discrete element simulations and experiments for 'sandpiles' composed of spherical particles. *Powder Technology* 160(3): 219-228.

LoCurto, G. J., X. Zhang, V. Zarikov, R. A. Bucklin, L. Vu-Quoc, D. M. Hanes, and O. R. Walton. 1997. Soybean impacts: experiments and dynamic simulations. *Transactions of the ASAE* 40(3):789-794.

Lorenzen, R. T. 1957. Effect of moisture content on mechanical properties of small grains. M.S. thesis. Davis, California: University of California-Davis.

McLelland, M. and Miller, N. 2001. Using 1,000 kernel weight for calculating seeding rates and harvest losses. Agdex 100/22-1. Available on http://www1.agric.gov.ab.ca/ $department/ deptdocs.nsf/ all/ agdex81? opendocument Accessed 13 April 2007.

Mindlin, R. 1949. Compliance of elastic bodies in contact. *Journal of Applied Mechanics* 16: 259-268.

Mindlin, R. D. and H. Deresiewicz. 1953. Elastic spheres in contact under varying oblique forces. *Transactions of ASME, Series E. Journal of Applied Mechanics* 20: 327-344.

Mirghasemi, A. A., L. Rothenburg, and E. L. Matyas. 2002. Influence of particle shape on engineering properties of assemblies of two-dimensional polygon-shaped particles. *Geotechnique* 52(3): 209-217.

Misra, R. N. and J. H. Young. 1981. A model for predicting the effect of moisture content on the modulus of elasticity of soybeans. *Transactions of the ASAE* 24(5): 1338-1341, 1347.

Mohsenin, N. N. 1986. *Physical Properties of Plant and Animal Materials*. 2nd ed. New York: Gordon and Breach Science Publishers.

Molenda, M. and J. Horabik. 2005. Characterization of mechanical properties of particulate solids for storage and handling. Part 1. In *Mechanical Properties of Granular Agro-Materials and Food Powders for Industrial Practice*. J. Horabik and J. Laskowski. eds. Lublin: Institute of Agrophysics Polish Academy of Sciences.

Mustoe, G. G. W. and M. Miyata. 2001. Material flow analyses of noncircular-shaped granular media using discrete element methods. *Journal of Engineering Mechanics* 127(10): 1017-1026.

Nelson, S. O. 2002. Dimensional and density data for seeds of cereal grain and other crops. *Transactions of the ASAE* 45(1):165-170.

Ng, T. T. 2001. Fabric evolution of ellipsoidal arrays with different particle shapes. *Journal of Engineering Mechanics* 127(10): 994-999.

O'Sullivan, C. and J. D. Bray. 2004. Selecting a suitable time step for discrete element simulations that use the central difference time integration scheme. *Engineering Computations* 21(2-4): 278-303.

Raji, A. O., and J. F. Favier. 2004a. Model for the deformation in agricultural and food particulate materials under bulk compressive loading using discrete element method, Part I: Theory, model development and validation. *Journal of Food Engineering* 64(3): 359-371.

Raji, A. O., and J. F. Favier. 2004b. Model for the deformation in agricultural and food particulate materials under bulk compressive loading using discrete element method, Part II: Compression of oilseeds. *Journal of Food Engineering* 64(3): 373-380.

Remy, B., J. G. Khinast, and B. J. Glasser. 2009. Discrete element simulation of free-flowing grains in a four-bladed mixer. *AIChE Journal* 55(8): 2035-2048.

Rothenburg, L., R. J. Bathurst. 1992. Micromechanical features of granular assemblies with planar elliptical particles. *Geotechnique* 42(1): 79-95.

Sawada, S. and T. B. S. Pradham. 1994. Analysis of anisotropy and particle shape by distinct element method. In *Computer Methods and Advancements in Geomechanics*, Vol. 1, 665-670. H. Siriwardane and M. M. Zaman, eds. Rotterdam, The Netherlands: Balkema.

Sharma, R. K. and W. K. Bilanski. 1971. Coefficient of restitution of grains. *Transactions of the ASAE* 14(2): 216-218.

Shelef, L., and N. N. Mohsenin. 1969. Effect of moisture content on mechanical properties of shelled corn. *Cereal Chemistry* 46(3): 242-253.

Shroyer, J. P., P. D. Ohlenbusch, S. Duncan, C. Thompson, D. L. Fjell, G.L. Kilgore, R. Brown, and S. Staggenborg. 1996. Kansas Crop Planting Guide. L-818. Manhattan, Kansas: Kansas State University Cooperative Extension Service.

Smith, C. E. and P. Liu. 1992. Coefficient of restitution. *Journal of Applied Mechanics* 59(4): 963-969

Stahl, B. M. 1950. Grain Bin Requirements. USDA Circular 835. Washington, D. C.: U.S. Department of Agriculture.

Stewart, B. R. 1968. Effect of moisture content and specific weight on internal-friction properties of sorghum grain. *Transactions of the ASAE* 11(2): 260-266.

Theuerkauf, J., S. Dhodapkar, and K. Jacob. 2007. Modeling granular flow using discrete element method – from theory to practice. *Chemical Engineering* 114(4): 39-46.

Thomas, P. A. and J. D. Bray. 1999. Capturing nonspherical shape of granular media with disk clusters. *Journal of Geotechnical and Geoenvironmental Engineering* 125(3): 169-178.

Ting, J. M., L. R. Meachum, and J. D. Rowell. 1995. Effect of particle shape on the strength and deformation mechanism of ellipse-shaped granular assemblages. *Engineering Computations* 12(2): 99-108.

Train, D. J. 1958. Some aspects of the property of angle of repose of powders. *Journal of Pharmacy and Pharmacology (Supplement)* 10: 127-135.

Tsuji, Y., T. Tanaka, and T. Ishida. 1992. Lagrangian numerical simulation of plug flow of cohesionless particles in a horizontal pipe. *Powder Technology* 71(3): 239-250.

Ullidtz, P. 1997. Modelling of granular materials using the discrete element method. In *Proceedings of the 8th International Conference on Asphalt Pavements*, Vol. 1, 757-769. August 10-14. Seattle, Wash.: University of Washington.

USDA GIPSA. 1996. Chapter 5: Test weight per bushel apparatuses. In *Equipment Handbook*. Washington, D.C.: USDA Grain Inspection, Packers, and Stockyards Administration, Federal Grain Inspection Service.

USDA GIPSA. 2004. *Grain Inspection Handbook, Book II, Grain Grading Procedures.* Washington, D.C.: USDA Grain Inspection, Packers, and Stockyards Administration, Federal Grain Inspection Service.

Vu-Quoc, L., X. Zhang, and O. R. Walton. 2000. A 3-D discrete element method for dry granular flows of ellipsoidal particles. *Computer Methods in Applied Mechanics and Engineering* 187(3-4): 483-528.

Walton, O. R. 1994. Effects of interparticle friction and particle shape on dynamic angles of repose via particle-dynamic simulation. Presented at the Workshop on Mechanics and Statistical Physics of Particulate Materials, June 8-10, La Jolla, Cal.

Walton, O. R. and R. L. Braun. 1993. Simulation of rotary-drum and repose tests for frictional spheres and rigid sphere clusters. In *Proceedings of DOE/NSF Workshop on Flow of Particulates and Fluids*, Sept. 29-Oct. 1, Ithaca, N.Y.

Watson, S. A. 2003. Chapter 3: Description, development, structure and composition of the corn kernel. In *Corn: Chemistry and Technology*. P. J. White and L. A. Johnson, eds. St. Paul, Minn.: American Association of Cereal Chemists, Inc.

Wightman, C., M. Moakher, F. J. Muzzio, and O. R. Walton. 1998. Simulation of flow and mixing of particles in a rotating and rocking cylinder. *AIChE Journal* 44(6): 1266-1276.

Yang, Y. and M. D. Schrock. 1994. Analysis of grain kernel rebound motion. *Transactions of the ASAE* 37(1): 27-31.

Zenz, F. A. 1957. How solid catalysts behave. *Petroleum Refiner* 36(4): 173-178.

Zhang, X. and L. Vu-Quoc. 2002. A method to extract the mechanical properties of particles in collision based on a new elasto-plastic, normal force-displacement model. *Mechanics of Materials* 34(12): 779-794.

Zhou, Y. C., B. H. Xu, A. B. Yu, and P. Zulli. 2002. An experimental and numerical study of the angle of repose of coarse spheres. *Powder Technology* 125(1): 45-54.

Zhou, Y. C., B. D. Wright, R. Y. Yang, B. H. Xu, and A. B. Yu. 1999. Rolling friction in the dynamic simulation of sandpile formation. *Physica A* 269(2-4): 536-553.